



HAL
open science

A repertoire of cationic and anionic conductances at the plasma membrane of *Medicago truncatula* root hairs

Limin Wang, Man-Yuan Guo, Jean-Baptiste Thibaud, Anne-Alienor Very, Hervé Sentenac

► To cite this version:

Limin Wang, Man-Yuan Guo, Jean-Baptiste Thibaud, Anne-Alienor Very, Hervé Sentenac. A repertoire of cationic and anionic conductances at the plasma membrane of *Medicago truncatula* root hairs. *The Plant Journal*, 2019, 98 (3), pp.418-433. 10.1111/tpj.14238 . hal-02122232

HAL Id: hal-02122232

<https://hal.science/hal-02122232>

Submitted on 10 Aug 2022

HAL is a multi-disciplinary open access archive for the deposit and dissemination of scientific research documents, whether they are published or not. The documents may come from teaching and research institutions in France or abroad, or from public or private research centers.

L'archive ouverte pluridisciplinaire **HAL**, est destinée au dépôt et à la diffusion de documents scientifiques de niveau recherche, publiés ou non, émanant des établissements d'enseignement et de recherche français ou étrangers, des laboratoires publics ou privés.



Distributed under a Creative Commons Attribution 4.0 International License

A repertoire of cationic and anionic conductances at the plasma membrane of *Medicago truncatula* root hairs

Limin Wang^{1,a}, Man-Yuan Guo¹, Jean-Baptiste Thibaud^{1,2}, Anne-Aliénor Véry^{1,*}, Hervé Sentenac¹

¹Biochimie & Physiologie Moléculaire des Plantes, UMR Univ Montpellier, CNRS, INRA, SupAgro, Montpellier, France

²Institut des biomolécules Max Mousseron, UMR 5247 CNRS-UM-ENSCM, Faculté de Pharmacie, 15 avenue Charles Flahault, BP 14491, F34093 Montpellier cedex 3, France

^aPresent address: Department of Plant Sciences, University of Cambridge, Downing Street, Cambridge CB2 3EA, United Kingdom

*For correspondence (e-mail: very@supagro.inra.fr)

Running title: *Medicago truncatula* root hair ionic conductances

Keywords: *Medicago truncatula*, root hair, K⁺, cation, Cl⁻ transports, patch-clamp

This article has been accepted for publication and undergone full peer review but has not been through the copyediting, typesetting, pagination and proofreading process, which may lead to differences between this version and the Version of Record. Please cite this article as doi: 10.1111/tpj.14238

This article is protected by copyright. All rights reserved.

SUMMARY

Root hairs, as lateral extensions of epidermal cells, provide large absorptive surfaces to the root, and are major actors of plant hydromineral nutrition. In contact with the soil, they also constitute a site of interactions between the plant and rhizospheric microorganisms. In legumes, initiation of symbiotic interactions with N₂-fixing rhizobia is often triggered at the root hair cell membrane in response to nodulation factors secreted by rhizobia, and involves early signaling events with changes in H⁺, Ca²⁺, K⁺ and Cl⁻ fluxes inducing transient depolarization of the cell membrane. Here, we aimed to build a functional repertoire of the major root hair conductances to cations and anions in the sequenced legume model *Medicago truncatula*. Five root hair conductances were characterized through patch-clamp experiments on enzymatically recovered root hair protoplasts. These conductances displayed varying properties in terms of voltage dependence, kinetics and ion selectivity. They consisted of hyperpolarization and depolarization-activated conductances for K⁺, cations or Cl⁻. Among them, one weakly outwardly-rectifying cationic conductance and one hyperpolarization-activated slowly inactivating anionic conductance were not known as active in root hairs. All five conductances were detected in apical regions of young growing root hairs, using membrane spheroplasts obtained by laser-assisted cell-wall microdissection. Combined with recent root hair transcriptomes of *M. truncatula*, this functional repertoire of conductances is expected to help the identification of candidate genes for reverse genetics studies to investigate the possible role of each conductance in root hair growth and interaction with the biotic and abiotic environment.

INTRODUCTION

Root hairs are outgrowths of the apical cells of the epidermis of plant roots, and play important functions in regulating water and nutrient uptake from the soil (Peterson *et al.*, 1996; Long, 1996). In legumes, they also play a crucial role in the establishment of a symbiotic interaction with nitrogen-fixing rhizobia (Fahraeus, 1957). During rhizobial infection, molecular cross-talk occurs between root hairs and rhizobia. Ionic exchanges across the root hair cell membrane, notably involving Ca²⁺, Cl⁻, K⁺ and H⁺, are amongst the earliest responses to the nodulation factors (NF) secreted by rhizobia (Felle *et al.*, 1998), creating calcium and electrical (by affecting the membrane potential) signals (Ehrhardt *et al.*, 1992; Felle *et al.*, 1995).

This article is protected by copyright. All rights reserved.

Despite their importance, the ion conductances from plant root hairs have been poorly investigated, when compared with those from guard cells for example, particularly *in situ*. Only a handful of papers have described ion channel currents in root hairs. Such information concerns mainly *Arabidopsis*. Lew (1991) recorded, by voltage-clamping *Arabidopsis* root hair cells using double-barreled microelectrodes, proton pump currents and potassium currents sensitive to the tetraethyl ammonium (TEA) blocker. By using the patch-clamp technique, Gassmann and Schroeder (1994) described an inwardly-rectifying K^+ conductance in root hairs of wheat. Then, by coupling reverse genetics to patch-clamp studies, Hedrich's group provided evidence that *Arabidopsis* root hair protoplasts are equipped with two K^+ inwardly rectifying Shaker channel subunits (AKT1 and AtKC1) and a K^+ outwardly rectifying one, GORK (Ivashikina *et al.*, 2001; Reintanz *et al.*, 2002). In addition, hyperpolarization-activated and depolarization-activated calcium channels were reported at the tip of *Arabidopsis* root hairs (Véry and Davies, 2000; Miedema *et al.*, 2008).

In leguminous plants, few analyses have investigated root hair ion channel activity. In *Medicago sativa*, beside Shaker-like inwardly and outwardly rectifying K^+ currents, an anionic current was detected by voltage-clamp on intact root hairs (Bouteau *et al.*, 1999; Kurkdjian *et al.*, 2000). The ion channels present in root hairs of *Medicago truncatula*, whose genome was recently sequenced, were not investigated so far at the functional level.

In this study, we describe five ionic conductances active at the plasma membrane of *Medicago truncatula* root hairs, their major functional properties being studied by the patch-clamp technique. The term “conductance” in our experiments made in a native context refers to a type of permeation pathway that can be mediated by a single molecular identity or by set of channels of several identities but displaying similar properties. Overall, this study of the ionic conductances of the root hair plasma membrane of *M. truncatula* is aimed at building a “repertoire”, which could help us progress in the identification of the main actors in nutrient uptake and in channel-mediated responses to biotic and abiotic signals in leguminous plants.

RESULTS

With the aim to identify the repertoire of main cationic and anionic conductances present at the plasma membrane of *Medicago truncatula* root hairs, root hair protoplasts were first recovered by enzymatic digestion of the apical cell wall of root hairs. This enabled to get a

large number of protoplasts, facilitating a detailed characterization by patch-clamp. Several types of conductances were identified, and those which were most often encountered were further characterized. Some were reminiscent of conductances already described in root hair cells from other plants (*e.g.*, Shaker-like conductances), whereas others have not been reported previously in root hair cells. The characterized conductances are described and compared below, sorted based on their sensitivity to voltage and ionic permeability, into three classes: cationic outwardly-rectifying, cationic inwardly-rectifying and anionic conductances.

Cationic outwardly-rectifying conductances

A first set of patch-clamp solutions were designed to investigate K^+ -permeable conductances in our root hair protoplasts. External and internal (pipette) solutions contained 30 mM and 150 mM K^+ respectively (Figure 1, Table S1). In order to discard anionic currents, low concentrations of permeant anions were used (2 and 4 mM Cl^- in external and internal solutions, respectively), by adding K^+ as a gluconate salt. The calcium concentration was set to 1 mM externally, and was buffered to a low value internally (free $Ca^{2+}_i < 10$ nM). The pH was 5.6 externally and 7.4 internally.

By applying a voltage-clamp protocol with a holding voltage at -75 mV, and 1.5 s-lasting pulses at less negative voltages varying with 15 mV increments up to +75 mV (Figure 1a), outward currents were mainly recorded. Several conductances were distinguished based on the level of rectification and current activation kinetics.

The conductance that was most often observed displayed weak outward rectification (Figure 1b, d). Upon application of depolarizing pulses, its currents comprised an instantaneous component and a time-dependent component, the relative part of the latter increasing with depolarization (Figure 1b). Current activation was smooth with exponential kinetics. The time constant of half activation determined at 45 mV was 67 ± 3 ms ($n=3$). Small deactivation currents were observed upon return to the holding voltage after the activation pulse (Figure 1b).

Besides this weakly rectifying conductance, a strongly outwardly-rectifying Shaker-like conductance was evidenced in the same experimental conditions (Figure 1c, e). This conductance displayed a typical slow sigmoidal activation of currents and slow deactivation kinetics upon return to the holding voltage (Figure 1c), recalling the kinetics of the Arabidopsis SKOR and GORK outward Shaker channels characterized in *Xenopus* oocytes and *in planta* (Gaymard *et al.*, 1998; Ache *et al.*, 2000; Ivashikina *et al.*, 2001; Hosy *et al.*,

2003). The time constant of half-activation of Shaker-like currents at 45 mV was 301 ± 58 ms ($n=3$), thus 4.5 times larger than that of the weakly-rectifying smooth conductance described above which is thereafter called by contrast “fast-activating” outward conductance.

The effect of varying the external K^+ concentration was examined on both the “fast-activating” and the Shaker-like outward conductances, using a set of external solutions containing K-gluconate concentrations at 3, 10, 30 or 100 mM, in the same background (1 mM $CaCl_2$ at pH 5.6). Decreasing the external concentration of K^+ shifted negatively the current-voltage (I-V) relationships of the “fast-activating” conductance, indicating that this conductance is permeable to K^+ (Figure 1f). This also increased the outward rectification of currents (Figure 1f), which appeared strong with 3 mM external K^+ , while almost absent with 100 mM external K^+ . To check whether the rectification involved a regulation by voltage of the corresponding conductance, a combined Goldman-Boltzmann equation was fitted to the mean steady-state I-V relationships (Véry *et al.*, 1995). This revealed that the observed rectification could be mostly explained by the transmembrane K^+ concentration gradient (Figure 1f). Only a slight voltage gating, not affected by the external K^+ concentration, had to be included to fully account for the shape of the I-V relationships (Figure 1h): the obtained activation curve upon depolarization displayed an apparent gating charge (z) of 0.17, and a half activation potential (E_{a50}) of 33 mV. In the Shaker-like conductance, in contrast to the “fast-activating” conductance, the outward rectification was strong whatever the external K^+ concentration (Figure 1g). Analysis of the Shaker-like gating by depolarization, fitting Boltzmann equations to the deactivation currents, indicated a large apparent gating charge z of 1.3, and E_{a50} values varying with the external K^+ concentration (Figure 1i). The E_{a50} variations followed those of the K^+ equilibrium potential (E_K), however with weaker slope (44 mV per 10 fold activity change; Figure 1i), as already reported for such type of conductance (Ache *et al.*, 2000; Langer *et al.*, 2002).

To explore in more details the selectivity of the two outward conductances, reversal potentials of currents were compared in the set of solutions containing varying external K^+ concentrations. A “tail current” protocol (Figure 2a) was used: in a first step, outwardly rectifying channels were opened by applying a positive voltage, then were progressively closed in less depolarized conditions flanking their reversal potential (Figure 2b, c). The reversal potential of both the Shaker-like and the “fast-activating” outward currents, graphically determined from time decreasing currents at the test voltages (Figure 2d, e), was identical to E_K in the presence of 100 mM external K^+ (Figure 2f, g). When the external K^+

concentration was decreased, the reversal potential remained close to E_K in the Shaker-like conductance (52 mV shift of E_{rev} per 10-fold change in external K^+ activity, as compared to 58 mV shift of E_K ; Figure 2g), while it clearly deviated from E_K in the “fast-activating” conductance (42 mV shift of E_{rev} per 10-fold change in external K^+ activity; Figure 2f). This indicates that the “fast-activating” conductance is less selective for K^+ than the Shaker-like outward conductance. The cationic selectivity of both conductances was further addressed by comparing reversal potentials in solutions containing 50 millimole.L⁻¹ of different monovalent cations (K^+ , Na^+ , Rb^+ , Li^+ or NH_4^+). The Shaker-like outward conductance showed selectivity for K^+ and Rb^+ , compared to the other cations (relative permeability to K^+ close to 0.3 for Na^+ , Li^+ and NH_4^+ ; Figure S1b, d). In contrast, the “fast-activating” outward conductance appeared fairly non-selective for the different cations (Figure S1a, c), since permeabilities to K^+ , Na^+ and Rb^+ were almost equal. This conductance displayed however a weak selectivity against Li^+ ($P_{Li}/P_K = 0.6 \pm 0.01$) and, surprisingly, a permeability to NH_4^+ larger than that to K^+ ($P_{NH_4}/P_K = 1.5 \pm 0.2$) (Figure S1a, c). At last, the sensitivity to pH of both outward conductances was examined. The outward current was slightly increased in the Shaker-like conductance when the external pH was more alkaline (7.5 versus 5.6) (Figure S1f) similarly as in the outward Shakers GORK and SKOR (Véry *et al.*, 2014). More alkaline pH also increased the outward current in the “fast-activating” conductance (Figure S1e).

Cationic inwardly-rectifying conductances

The presence of inwardly-rectifying K^+ /cationic conductances in *M. truncatula* root hair plasma membrane was explored using dedicated protocols starting at a weakly negative holding voltage at which this type of conductance would be closed, then applying hyperpolarizing pulses to activate the conductance (Figure 3a, top).

As previously observed in root hairs from different species, a Shaker-like inwardly rectifying K^+ conductance (Gassmann and Schroeder, 1994; Bouteau *et al.*, 1999; Downey *et al.*, 2000; Hartje *et al.*, 2000) was present in the enzymatically-recovered root hair protoplasts. An example of corresponding current traces and I-V plot obtained with 30 mM K-gluconate and 10 mM $CaCl_2$ (at pH 5.6) in the external solution and 150 mM K-gluconate (at pH 7.4) in the internal solution is shown in the bottom panel of figure 3a. The inwardly-rectifying conductance was observed upon membrane hyperpolarization from a threshold of about -120 mV (Figure 3b) and displayed the typical slow activation of inward Shaker currents, and fast exponential deactivation when the membrane was weakly polarized

again (Figure 3a; Zimmermann *et al.*, 1998; Hartje *et al.*, 2000; Reintanz *et al.*, 2002; Geiger *et al.*, 2009a). Steady-state currents of the *M. truncatula* root hair Shaker-like inward conductance were strongly rectifying (Figure 3b), as classically observed for this conductance type. Half saturation (apparent K_M) of this inward conductance upon increasing the external K^+ concentration occurred at about 34 mM K^+ (Figure S2).

Since the Shaker-like conductance displayed inward rectification, its selectivity was addressed using “tail current” protocols (Figure 4a), with first activation of the conductance at a quite negative voltage before applying less negative test voltages, for determination of the conductance reversal potential. The analysis of tail currents in the 30 mM K^+ and 10 mM $CaCl_2$ -containing external solution gave an E_{rev} value only 3 mV positive to E_K (Figure 4a, b). Varying the external K^+ concentration from 3 to 100 mM (in 1 mM $CaCl_2$ background to avoid blockage of the conductance at low external K^+ concentration), E_{rev} values closely followed changes of E_K , shifting by 52 mV upon 10-fold change in the external K^+ activity (Figure 4c). Thus, in the tested solutions both with 1 or 10 mM external Ca^{2+} and varying Cl^- backgrounds, the inwardly rectifying Shaker-like conductance was confirmed to mainly carry, as expected, K^+ ions.

Two types of “Slow” anion conductances

For the characterization of the anion conductances at the plasma membrane of *M. truncatula* root hairs, in order to prevent K^+ channel activity recording, TEA-Cl and/or $CaCl_2$ -based patch-clamp solutions without added K^+ were used. A first set of solutions resulted in almost symmetrical Cl^- concentrations on both sides of the membrane: 100 mM at the external face of the membrane and 113 mM at the internal face. The free Ca^{2+} concentration of the internal solution was buffered to 1 μM (Table S1). Using these solutions and voltage-clamp protocols composed of a positive holding potential (set at 0 to +20 mV), and 10-s voltage pulses from positive to quite negative values in -15 or -30 mV increments (Figure 5a, b), two types of anion conductances were dominant.

One of these two anion conductances mediated currents that were reminiscent of those elicited by S-type anion conductances described in different plant tissues, including roots and guard cells in different species (Schroeder and Keller, 1992; Frachisse *et al.*, 2000; Roberts, 2006; Geiger *et al.*, 2009b & 2011). This root hair conductance, which was steadily active at the 0 mV holding potential used in our experiments, showed typical slow deactivation of currents upon prolonged application of hyperpolarizing pulses (Figure 5c). Thus, currents

elicited by this conductance type were maximal at the beginning of the hyperpolarizing pulse and decreased during the pulse, more so and faster when the voltage pulse became more negative (Figure 5c). Current-voltage relationships determined at the end of the 10-s voltage pulses displayed a maximal negative current (anion efflux) at about -175 to -200 mV, in the 100/113 external/internal mM Cl⁻ conditions (Figure 5e). At more negative voltages, the current at the end of the pulse was only slightly reduced. The relative open probability of this conductance ($P_o/P_{o,max}$), whose voltage dependence was analyzed by dividing, for each applied voltage, the steady state current by the driving force, decreased upon hyperpolarization. Using simple Boltzmann functions to describe the regulation by voltage of the S-type conductance open probability, provided good fits to the I-V data (Figure 5e) and allowed to extract an activation curve (Figure 5g) reminiscent of those provided for guard cell S-type channels (Geiger *et al.*, 2011), with a small apparent gating charge ($z = 0.2$) and a quite negative half activation potential ($E_{a50} = -158$ mV). The reversal potential of this S-type conductance, directly determined from I-V relationships in these ionic conditions with Cl⁻ as dominant anion species was close to E_{Cl} (Figure 5e).

Other root hair protoplasts displayed another kind of anion current pattern with major kinetic differences compared to the above described classical S-type conductance. Actually, upon application of hyperpolarization pulses from a slightly positive holding potential, the initial negative current was not maximal (especially when applying the most negative voltage pulses). Indeed, the current slowly increased at the beginning of the hyperpolarization pulse (Figure 5d). This suggested that hyperpolarization activated this conductance. Additionally to this voltage dependent activation, a voltage-dependent inactivation was observed. This was visible when pulses were applied at voltages more negative than *ca* -130 mV, in which case a prolonged hyperpolarization led after the initial increase in current to a subsequent current decrease. The reduction of current initiated faster and was stronger when the applied voltage was more negative (Figure 5d). Thus, from the voltage threshold where current inactivation was detected, a peak of current was apparent during the 10-s pulses. I-V relationship at the end of the 10-s pulse displayed a marked maximum of negative current at about -150 mV (Figure 5f). At voltages less negative than -130 mV for which no late current decrease was observed, the slope of the I-V relationship increased with more negative voltages (Figure 5f), in contrast with that of the S-type conductance (Figure 5e). The activation curve of the hyperpolarization-activated conductance extracted from peak currents (Figure 5h) was almost opposite to that of the Medicago root hair S-type conductance, with similar apparent gating charge ($z = 0.2$) but opposite voltage gating, and half activation potential around -40 mV

(Figure 5g, h). The steady state current reversed very close to E_{Cl} (+ 3 mV; Figure 5f), suggesting that the slow hyperpolarization-activated conductance mediated anionic currents.

Changing the external Cl^- concentration from 100 to 20 mM (which made a 39 mV positive shift in E_{Cl}) induced a positive shift in the I-V relationships of both S-type and slow hyperpolarization-activated conductances (Figures 6a, b and S3). The mean shift in E_{rev} was 32 mV in the S-type and 38 mV in the slow hyperpolarization-activated conductance (Figure 6c, d). This confirmed that both conductances were Cl^- conductances.

The relative permeabilities to nitrate and chloride were compared in the slow hyperpolarization-activated conductance by replacing the external Cl^- (20 mM) with the same concentration of NO_3^- (0.5 mM $CaCl_2$ were however kept; Figure S4a, b). Current-voltage relationships showed a positive shift when NO_3^- replaced Cl^- (Figure S4c), the mean reversal potential shifting from $+25 \pm 2$ mV to $+47 \pm 4$ mV ($n = 5$). This indicated that the slow hyperpolarization-activated conductance was more permeable to Cl^- than to NO_3^- , with a relative permeability $P_{NO_3^-}/P_{Cl^-}$ of 0.4 (Figure S4d). This feature contrasts with reports concerning the S-type anion conductance described *in vivo* at the guard cell plasma membrane and the cloned S-type guard cell SLAH3 channel (Schmidt & Schroeder, 1994; Barbier-Brygoo *et al.*, 2000; Roberts *et al.*, 2006; Geiger *et al.*, 2011). This latter conductance was more often observed than the S-type one (in > 70% of ca. 25 protoplasts displaying one of these two conductances).

Effect of the cytosolic Ca^{2+} concentration on the activity of the cationic conductances

Ca^{2+} represents an important second messenger in root hair cells, in legumes in interaction with rhizobia in particular (Long, 1996). Large tip-base variations of cytosolic Ca^{2+} in root hairs also support tip growth (Felle *et al.*, 1997). We examined whether cytosolic Ca^{2+} affected the three cationic conductances observed in *M. truncatula* root hair protoplasts, i.e., the inward and outward Shaker-like conductances and the “fast-activating” outward cationic one. Using a pipette solution with the free Ca^{2+} concentration increased to 1 μ M, the three cationic conductances were still observed in the protoplasts (Figure 7a to 7c). However, the mean current was reduced in the two Shaker-like conductances, as compared to low cytosolic Ca^{2+} conditions (Figure 7d, e), by ca. 40% for the inward Shaker and 65% for the outward Shaker. The inward Shaker current decrease was accompanied by a slight negative shift (-15 mV) in the threshold of activation. The reversal potentials of currents of both the inward and outward Shaker conductances (-33 ± 3 and -27 ± 2 mV, respectively; $n = 3$) were similar to

those recorded at low cytosolic Ca^{2+} , remaining close to E_K , as expected for these highly K^+ -selective conductances. In contrast to the Shaker conductances, the fast-activating cationic outward conductance was enhanced by the high cytosolic Ca^{2+} concentration, by ca. 50% (Figure 7f). The apparent outward rectification was reduced, as compared to low cytosolic Ca^{2+} conditions (Figures 1b, d and 7c, f), and the reversal potential of currents (-18 ± 3.5 mV) was positively shifted by ca. 15 mV. This shift in E_{rev} may denote a permeability to Ca^{2+} in this weakly selective cationic conductance. A Cl^- contribution to the current mediated by this conductance could also be possible and contribute to the shift in E_{rev} . Indeed, E_{Cl} was shifted by +28 mV in the experiments with high internal Ca^{2+} , and weakly-selective cation conductances described in other plant species were reported to display significant permeability to Cl^- in addition to monovalents and Ca^{2+} (Wegner and de Boer, 1997; Zhang *et al.*, 2000 & 2002).

Co-occurrence of the different K^+ conductances in *M. truncatula* root hair protoplasts

Among the five characterized conductances in our root hair protoplasts, the K^+ -permeable ones (the “fast-activating” outward conductance and the outward and inward Shaker-like ones) could be evidenced using the same internal solutions, which rendered the analysis of co-occurrence of these three conductances possible with the aim to test the hypothesis of a preferential co-occurrence or of a mutual exclusion. Recordings obtained at low internal Ca^{2+} (Figure 8) were more particularly analyzed, since a larger number of recordings (104 protoplasts) were available in this condition.

Regarding the outward K^+ -permeable conductances, the fast-activating outward type was the predominant one. It was found in 56 of the 104 protoplasts examined (from which 29 displayed the inward Shaker-type conductance and 27 did not display this latter conductance), thus in ca. 55% of the protoplasts. The Shaker-like outward type was on the other hand observed in 24 protoplasts (12 displaying the inward Shaker-type conductance and 12 not displaying this conductance), thus in ca. 30% of the protoplasts. The presence of both types of outward conductances was only occasional, observed in only ~9% of protoplasts (in 8 of the 104 protoplasts). Altogether, these results provide evidence that the fast-activating outward conductance is rather rarely present together with the Shaker-like outward conductance, i.e. that these two conductances tend to be mutually exclusive from each other. In ca. 15% of the protoplasts (16 protoplasts in total out of the 104), neither of the two outward K^+ conductances was observed. In that latter case, the protoplasts either displayed an

instantaneously-activating outwardly-rectifying conductance or a "leak-like" (i.e. "Ohmic") K^+ one (conductances not further characterized).

The inwardly rectifying Shaker-like K^+ conductance was found to dominate the membrane conductance to K^+ in 56 from the 104 protoplasts, i.e., in 54% of the root hair protoplasts (Figure 8). Amongst these 56 protoplasts, the fast-activating outward K^+ conductance and the Shaker-like outward conductance dominated the membrane outward conductance to K^+ in 29 and 12 protoplasts, respectively, thus in ca. 52% and 22% of these protoplasts. Similar percentage (56% and 25%, respectively) were found among the 48 protoplasts sorted as displaying no inwardly rectifying Shaker-like K^+ conductance. Hence, no correlation appeared between the presence of the inward Shaker conductance and that of the outward ones.

The analysis of 16 protoplasts patch-clamped at high cytosolic Ca^{2+} (Figure S5) suggested that the same conclusions could be drawn: the fast-activating cationic conductance and the outward Shaker-type one dominated the outward conductances, the fast-activating cationic one being the most often encountered. Co-occurrence of the two outward conductances was rare (1 out of 16 protoplasts). The inward Shaker type dominated the inward conductances and was observed jointly with either the outward Shaker type (in 75% of protoplasts displaying this outward Shaker conductance: 3 out of 4 protoplasts) or the fast outward conductance (in ca. 60% of protoplasts displaying this fast conductance: 5 out of 8), confirming with high cytosolic Ca^{2+} , the absence of correlation between the presence of inward Shaker conductance and that of the cationic outward ones.

Conductances active in apical membrane of young root hairs

With the aim to investigate whether the characterized root hair conductances were active at the tip of young growing root hairs, the laser cell-wall ablation technique was used (Véry and Davies, 2000). The cell-wall of selected growing root hairs was burnt at the apex by the laser after a short plasmolysis of the cells, allowing the recovery of spheroplasts of apical membrane extruding from the cut wall upon deplasmolysis (Figure 9A). These spheroplasts were analyzed in the whole-cell configuration in the same ionic conditions and with the same voltage-clamp protocols as those used in the previous patch-clamp experiments on enzymatically-recovered protoplasts. The main conductances characterized in enzymatically-recovered protoplasts, i.e., the outwardly and inwardly rectifying Shaker-like ones, the fast-activating outward cationic one—and the two slow anionic ones (Figures 1b, c,

3a and 5c, d), were identified from their typical kinetics and I-V relationships in laser-obtained root hair spheroplasts (Figure 9b to 9f). This provided evidence that all the conductances characterized in enzymatically-recovered protoplasts were present in the apical membrane of growing root hairs.

DISCUSSION

The identified “repertoire” of *M. truncatula* root hair conductances compared to that of other plant cell types

An important number of plasma membrane plant conductances have already been characterized in varying cell types (Hedrich, 2012). However, integrative descriptions of the plasma membrane conductance equipment are still lacking for most cell types, except for guard cells, the main model of membrane transport biology in plants so far, in which a number of native plasma membrane conductances have been characterized since the 1980's, first in *Vicia faba* then in *Arabidopsis* (Ward *et al.*, 2009), and to a lesser extent for xylem parenchyma cells in barley (Köhler, 2007). Here, our aim was to build a repertoire of the major K⁺ and Cl⁻ conductances active at the plasma membrane of root hairs in the sequenced model legume *Medicago truncatula*.

Five root hair conductances from *M. truncatula* were characterized in this study. Among them, three are reminiscent of conductances described at the root hair membrane of other species. These conductances are the common K⁺ Shaker-like inwardly and outwardly rectifying ones (Fig. 1c and 3a; Véry *et al.*, 2014), already described in root hair cells from, e.g., *Arabidopsis* or *Medicago sativa* (Bouteau *et al.*, 1999; Ivashikina *et al.*, 2001; Reintanz *et al.*, 2002), and the S-type anion conductance observed for instance in root hairs from bean (Figure 5c; Dauphin *et al.*, 2001).

The kinetics, voltage threshold of activation, sensitivity to external K⁺ and affinity for K⁺ of the *M. truncatula* root hair inwardly rectifying Shaker-type conductance (Figure 3, Figure S2) are similar to those of counterparts described in root hairs from other plant species (Gassmann and Schroeder, 1994; Bouteau *et al.*, 1999; Reintanz *et al.*, 2002). Similarly, the kinetics, voltage gating, sensitivity to external K⁺ of the *M. truncatula* Shaker-like outward conductance (Figure 1 c, g, i) are fully consistent with the results from *in situ* analyses on similar root hair conductances in other species or with data obtained in *Xenopus* oocytes for the *Arabidopsis* GORK Shaker channel, which displays expression in root hairs (Bouteau *et*

Accepted Article
al., 1999; Ache *et al.*, 2000; Ivashikina *et al.*, 2001). On the other hand, none of these studies provided a detailed analysis of the cationic selectivity of any root hair Shaker-type outward conductance. The present analysis indicates that the ionic selectivity of the *M. truncatula* root hair Shaker-type conductance (Figure 2g, Figure S1b, d) is quite similar to that determined, by using the *Xenopus* oocyte expression system, for the Arabidopsis outward Shaker SKOR, which is specifically expressed in the root stele (Gaymard *et al.*, 1998; Johansson *et al.*, 2006).

Plasma membrane “slowly-inactivating” anion conductances, although reported in various cell types including root hairs (Frachisse *et al.*, 2000; Köhler and Raschke, 2000; Dauphin *et al.*, 2001; Zhang *et al.*, 2004a; Hosy *et al.*, 2005; Mori *et al.*, 2006), have so far mainly been analyzed (by patch-clamp or *in situ* voltage-clamp) at the membrane of guard cells (Schroeder and Keller, 1992; Forestier *et al.*, 1998; Vahisalu *et al.*, 2008, Geiger *et al.*, 2009b; Guzel Deger *et al.*, 2015). Here, two slow anion conductances manifested themselves at the plasma membrane of *M. truncatula* root hairs. From current kinetics and shape of I-V relationships (Figure 5c to 5f), one of the two anion conductances of *M. truncatula* resembled S-type conductances described in the literature (Köhler and Raschke, 2000; Mori *et al.*, 2006), and in particular the one previously identified in root hairs of bean (*Phaseolus vulgaris*) subjected to hydric stress (Dauphin *et al.*, 2001).

The second slowly inactivating type of anion conductances, which was the most frequently observed anionic conductance in *M. truncatula* root hair protoplasts in our experimental conditions, is reminiscent (to our knowledge) of only one Cl⁻ conductance described so far, that in pea mesophyll cells (Elgenza and Volkenburgh, 1997; Roberts, 2006). From its slow kinetics of current inactivation along 10-s hyperpolarization pulses (Figure 5d), it may be classified in the slow-type anion conductances. However, the general shape of its I-V relationships at steady-state was quite different from that of S-type channels, more closely resembling that of rapid-type conductances (Figures 5f, 6b, S3 and S4; Frachisse *et al.*, 1999; Vahisalu *et al.*, 2008; Diatloff *et al.*, 2010; Roelfsema *et al.*, 2012). Furthermore, a distinctive feature of this *M. truncatula* root hair anion conductance, displayed also by the pea mesophyll conductance described by Elgenza and Volkenburgh (1997), is that, upon hyperpolarization, the current first displays a slow activation before inactivating (Figures 5d and S3). Thus, this conductance seems better described as a hyperpolarization-activated slowly inactivating one, conversely to S-type (depolarization-activated) conductances. Hyperpolarization-activated anion conductances displaying no or slow inactivation of currents have been reported (Kurkdjian *et al.*, 2000; Zhang *et al.*, 2004a; Roberts, 2006).

This article is protected by copyright. All rights reserved.

They however all display instantaneous current activation upon membrane hyperpolarization, with the exception of the pea mesophyll conductance (Elgenza and Volkenburgh, 1997), which shares with the *M. truncatula* conductance slow initial activation of currents upon hyperpolarization. Thus, from kinetics of current activation/inactivation, the hyperpolarization-activated *M. truncatula* root hair and pea mesophyll anion conductances could be considered as a particular type of hyperpolarization-activated anionic conductances which might be legume-specific. Finally, it should be noted that the *M. truncatula* hyperpolarization-activated conductance, besides its original kinetic properties, also displayed an unusual selectivity, showing higher permeability to Cl^- than to NO_3^- (Figure S3). This contrasts with the commonly reported higher NO_3^- to Cl^- permeability of anion conductances (S-type, rapidly inactivating and hyperpolarization-activated ones) in many cell types and with the first cloned anion channels characterized in heterologous system (Hedrich and Marten, 1993; Schmidt and Schroeder, 1994; Roberts, 2006; Geiger *et al.*, 2009b & 2011; Guterath *et al.*, 2013; Maierhofer *et al.*, 2014). Thus, the characterization of this *M. truncatula* anion conductance represents a particularly interesting contribution to our knowledge of plant anion channel diversity.

The last conductance of the present *M. truncatula* root hair “repertoire”, the fast-activating outwardly-rectifying cation conductance, weakly selective among cations, had not been previously reported in root hair cells, but is reminiscent of conductances already described in other cell types. A variety of depolarization-activated non-selective cation channels have been reported in the literature: e.g., in xylem parenchyma (Wegner and Raschke, 1994; Wegner and de Boer, 1997), *Arabidopsis* root / root epidermis (Demidchik and Tester, 2002; Shabala *et al.*, 2006), *Arabidopsis* and *Thlaspi* mesophyll (Piñeros & Kochian, 2003; Shabala *et al.*, 2006), bean seed coat and cotyledon dermal cells (Zhang *et al.*, 2000, 2002 & 2004b). In all these studies, a fast or ‘instantaneous’ kinetics of current activation was observed. The reported conductances were mostly depicted as only weakly more permeable to cations than to anions, with $P_{\text{cation}}/P_{\text{Cl}}$ in the range of 2 to 4 (Wegner and de Boer, 1997; Zhang *et al.*, 2000 & 2002), and weakly discriminating among monovalent cations. The *M. truncatula* fast-activating outwardly-rectifying conductance displayed strong similarity, with respect to cation selectivity and voltage dependence, with a weakly voltage-dependent non selective cation channel described in wheat roots (Davenport and Tester, 2000). Both conductances poorly discriminated among monovalent cations and displayed the highest permeability to NH_4^+ and the lowest one to Li^+ (Figure S1). The *M. truncatula* fast-activating outward conductance is also reminiscent of the weakly cationic-selective NORC conductance of

barley root xylem parenchyma permeable to both monovalents and Ca^{2+} (Wegner and Raschke, 1994; Wegner and de Boer, 1997). Analysis of the regulation by voltage of NORC in xylem parenchyma cells indicated in contrast to the Shaker-like conductance, a non- K^+ -dependent gating, and a smaller gating charge than that in Shakers (~2.5 fold smaller; Wegner and de Boer, 1997). The voltage-gating of the *M. truncatula* fast-activating conductance was also non- K^+ -dependent, and the gating charge was very low (Figure 1h), the observed rectification being mostly explained by transmembrane concentration gradients (Figure 1f).

Gene candidates for the characterized ionic conductances from *M. truncatula* root hairs

Based on RNA-seq analysis of the *M. truncatula* root hair transcriptome from plants grown in the same experimental conditions as those used for the present electrophysiological analyses (Damiani *et al.*, 2016), molecular correspondence for some of the macroscopic conductances evidenced in root hair protoplasts can be proposed (Figure 10). Since Medtr5g077770 is the unique outward Shaker gene present in the genome of *M. truncatula* and is expressed in root hairs (Damiani *et al.*, 2016), it certainly encodes the Shaker outwardly rectifying K^+ conductance of the root hair membrane. Regarding the inwardly-rectifying Shaker K^+ conductance, the candidate genes are Medtr3g108320 and Medtr4g113530, which are homologous to *AtKCI* and *AKT1* genes in Arabidopsis, and are both expressed in *M. truncatula* root hairs (Damiani *et al.*, 2016). In Arabidopsis, both AKT1 and AtKC1 Shaker subunits contribute to the root hair inward K^+ conductance (Reintanz *et al.*, 2002; Wang *et al.*, 2010). AtKC1 is unable to form by itself functional inward channels at the plasma membrane but associates with AKT1 in heteromeric channels (Reintanz *et al.*, 2002; DUBY *et al.*, 2008). Thus, as in Arabidopsis, the inward Shaker-type conductance in *Medicago* is likely composed of both MtAKT1 homomeric channels and MtAKT1/MtKC1 heteromers.

The molecular identity is much more speculative for the outwardly rectifying weakly selective conductance found in *M. truncatula* root hairs. Several gene families have been proposed to encode weakly selective plasma membrane cation channels, the most frequently proposed ones being the CNGC, GLR, annexin, MCA and OSCA families (Demidchik *et al.*, 2002; White *et al.*, 2002; Jammes *et al.*, 2011; Yuan *et al.*, 2014). Transporters from the KUP/HAK/KT family also are known as weakly selective cationic transport systems (Véry *et al.*, 2014) and KUP/HAK/KT members have been proposed to mediate cation effluxes *in vivo* (Osakabe *et al.*, 2013). Their selectivity between the monovalents K^+ , Na^+ and Li^+ is however

not well determined and transporters are believed to give rise to low current levels when compared to channels. Channel members from the families proposed to encode weakly selective plasma membrane cation channels have been suggested through *in planta* genetic analyses to be involved in different cation transports including that of Ca^{2+} (Ali *et al.*, 2007; Laohavisit *et al.*, 2012; Wang *et al.*, 2013; Kong *et al.*, 2016), but their electrophysiological properties have not been extensively characterized. *Medicago* annexin 1 (Medtr8g038210), coding for one of the six annexins present in root hairs (de Carvalho-Niebel *et al.*, 1998; Figure 10), has been shown to conduct cations across planar bilayer membrane (Kodavali *et al.*, 2013). However, lack of information on MtAnn1 regulation by voltage prevents comparison with the cationic conductances characterized in the present study. *M. truncatula* RNA-seq data indicate that root hairs expressed a large number of genes from CNGC, GLR and annexin families (Figure 10). Genes from these families could be proposed as molecular candidates of the weakly outwardly rectifying cationic conductance of *M. truncatula* root hairs.

The characteristic S-type anion conductance found in *M. truncatula* root hair protoplasts, based on its current kinetics and voltage gating (Figure 5c, e, g and 9e), is likely encoded by one or several of the 3 *SLAC* genes (Geiger *et al.*, 2009b & 2011) expressed in *Medicago* root hairs (Damiani *et al.*, 2016; Figure 10). On the other hand, the molecular identity of the hyperpolarization-activated slowly inactivating Cl^- conductance found in *M. truncatula* root hair protoplasts is more difficult to predict. The shape of its I-V relationship is reminiscent of that of R-type conductances, among which the Arabidopsis guard cell one has been attributed to the malate transporter AtALMT12 (Meyer *et al.*, 2010). R-type conductances and AtALMT12 are however endowed with fast kinetics of current activation/deactivation/inactivation and are activated by membrane depolarization (Thomine *et al.*, 1995; Meyer *et al.*, 2010; Mumm *et al.*, 2013) in contrast to the *M. truncatula* hyperpolarization-activated anion conductance (Figure 5d, f and h). This *M. truncatula* anion conductance also contrasts with cloned plasma membrane anion channels from *SLAC* and *ALMT* families by a higher permeability to Cl^- than to NO_3^- (Piñeros *et al.*, 2008; Zhang *et al.*, 2008; Geiger *et al.*, 2009b; Geiger *et al.*, 2011; Ligaba *et al.*, 2012). Thus, if this conductance was encoded by members from *SLAC* or *ALMT* gene families, this would indicate that a large functional diversity, beyond what is presently known, exists within these families.

Conclusion

Five *M. truncatula* root hair conductances were identified in enzymatically obtained protoplasts, two of which having no reported counterparts in root hairs from other plant species. The fact that all these conductances could be also recorded in root hair spheroplasts obtained using a laser assisted procedure provides evidence that their presence in enzymatically obtained protoplasts does not result from artefactual gene expression during the cell wall digestion but that they are actually active at the root hair cell membrane. Detection of their presence in our root hair spheroplasts also indicates that they can be active at least in the root hair apical region, involved in tip growth as well as in biotic interactions (e.g., with nitrogen-fixing rhizobia). The three cationic conductances were observed at both low and high cytosolic Ca^{2+} conditions and their activity was regulated by the internal Ca^{2+} concentration, indicating that they could play a role in varying physiological conditions. The fact that the two outwardly rectifying K^+ conductances characterized in the enzymatically obtained protoplasts are mutually exclusive from each other is compatible with the hypothesis that the enzymatic procedure provides a mix of protoplasts from root hairs at different developmental stages, displaying distinctive conductance equipment and/or distinctive cytosolic conditions, which would differentially modulate ion channel activities and would not be reversed during the patch-clamp experiments. The fact that the Shaker-type inwardly rectifying K^+ conductance can be either present in, or absent from, the protoplasts is also compatible with the above hypotheses.

The present report provides the most documented conductance “repertoire” for root hair cells. Members from this repertoire can be expected to play a role in plant mineral nutrition and/or mechanisms involved in root hair tip growth (e.g., via turgor regulation) or in various signaling events. For instance, they might be involved in the ionic responses to Nod factors secreted by rhizobia, known to rapidly trigger (within 1 or 2 min) changes in Ca^{2+} , Cl^- and K^+ fluxes leading, along with changes in H^+ fluxes, to electrical and calcium signaling events that constitute the earliest responses identified so far to Nod factors (Felle *et al.*, 1998). In the sequenced legume *M. truncatula*, the molecular identity of several members of the characterized repertoire could be hypothesized, which can pave the way to future analysis through reverse genetics of the role of these conductances in the multiple physiological functions of root hairs.

EXPERIMENTAL PROCEDURES

Plant cultivation

M. truncatula A17 (cv. Jemalong A17) was used in this study. Seeds were placed in a small container and chemical scarification was performed by soaking them in pure sulfuric acid for around 8 minutes. All H₂SO₄ liquid was then carefully removed. Seeds were washed several times with chilled water to avoid heating damage. Finally, the seeds were immersed in clean water for 1.5-2h. Then, the scarified seeds were sterilized by immersion for 3 minutes in a bleach 6% solution and were rinsed with sterile water several times. Sterilized seeds were transferred onto an agar Petri-dish (0.5 % (w/v) in deionized water) and kept in the dark at 4°C in order to break dormancy and get a synchronization of germination. Two days later, the plate was move to a growth chamber at 21°C for germination for 15 to 24 h. Seedlings (~9) were transferred to a square Petri dish of solid Fahraeus medium, overlaid by an autoclaved filter paper. The medium (modified from Vincent, 1970) contained 10 g/L of purified agar (Euromedex) and 0.5 mM MgSO₄, 0.7 mM KH₂PO₄, 0.8 mM Na₂HPO₄, 1 mM CaCl₂, 20 μM Fe-citrate, and 0.1 mg/L of MnSO₄, CuSO₄, ZnSO₄, H₃BO₃ and Na₂MoO₄. The pH was adjusted with KOH to 7.5. The lower part of the plate was wrapped in aluminum foil. The plate was placed at 25°C in a growth chamber.

Enzymatic isolation of root hair protoplasts

Three root apical portions of 3-4 cm were cut from 7 to 12 day-old seedlings grown on Fahraeus solid medium, and were incubated in an enzyme solution containing 1% (w/v) cellulase RS (Onozuka, Japan), 0.5% (w/v) macerozyme R-10 (Onozuka, Japan), 0.1% (w/v) pectolyase Y23 (Seishin Pharmaceutical, Japan), 1 mM CaSO₄, 25 mM MES and 250 mM D-sorbitol, in which the pH was adjusted to 5.5 by addition of KOH. During the digestion, the cell wall at the tip of the root hairs was first digested and protoplasts appeared at the tip of root hair. The follow-up of the cell-wall digestion and protoplast release under the microscope enabled to confirm the root hair origin of recovered protoplasts. After 1h and 20 min of digestion at 28°C with shaking at 60 rpm, the released protoplasts were filtered through a 40 μm nylon mesh and washed twice with the enzyme free medium after slow-speed centrifugation at 4°C. Finally, the protoplasts were re-suspended in the enzyme free medium and stored in the dark at 4°C until patch-clamp measurements were made.

Isolation of spheroplasts of apical root hair membrane by laser microdissection

Two day-old seedlings were used. Plasmolysis of root hairs was necessary prior to laser cell-wall cutting in order to prevent cell membrane damage by the laser energy (Figure 9a; Véry and Davies, 2000). Root hair plasmolysis was achieved within 3 min by using a solution containing 350 mM sorbitol and 5 mM CaCl₂. 0.2% Fluostain I (Sigma), a cell-wall binding dye absorbing UV light, was added to the plasmolysis solution in order to potentiate the action of the UV laser pulses on the cell wall. After cutting the apical cell-wall of a few root hairs with the laser (up to 7 min), another solution with lower osmolarity (200 mM sorbitol) was added to the chamber for root hair deplasmolysis (achieved within 1-3 min). During deplasmolysis, a rapid extrusion of spheroplasts of apical membrane out of holes made in root hair cell-wall was observed (Figure 9a). Root hair spheroplasts were excised by shaking the chamber. Batches of root hair spheroplasts (total number < 10) for patch-clamp experiments were renewed every hour.

Whole-cell patch clamp

Patch-clamp experiments were performed in the whole-cell configuration. Patch-clamp pipettes were pulled using a DMZ-Universal Puller (Zeitz-Instruments GmbH, Germany) from borosilicate capillaries (GC150F-7.5; Phymep, France) and fire polished (by the DMZ-Universal Puller). Microelectrode resistance was about 10 MOhms in experimental solutions. A reference Ag/AgCl half-cell completed the circuit. The patch clamp amplifier was an Axopatch 200B (Axon Instruments Inc., USA). Currents passing through the protoplast/spheroplast membrane were measured at least 5 min after seal formation and obtaining the whole-cell configuration, in order to allow the pipette solution to diffuse and control the protoplast cytosol ionic composition. Data were sampled at 1 kHz. The Clampex module of the pClamp9 software (Axon Instruments Inc., USA) was used for design of voltage-clamp pulse protocols and data (applied voltages and resulting currents) acquisition. Analysis was performed using the Clampfit module of pClamp10 and SigmaPlot 11 (Systat Software Inc., USA). Applied voltages were corrected for liquid junction potentials. Main pipette solutions designed for the characterization of the different ionic conductances are given in Table S1. Details on bath solutions are given in the result section.

Voltage gating, affinity and selectivity analysis

Voltage gating parameters (z : apparent gating charge, E_{a50} : half activation potential) were obtained through Boltzmann fits to initial deactivation currents (I_{tail}) upon return to a voltage where the channel open probability was nil ($I_{tail} = I_{tailmax}/(1+\exp(z*F(V-E_{a50})/R/T))$ in inwardly-rectifying conductances or $I_{tailmax}/(1+\exp(z*F(-V+E_{a50})/R/T))$ in outwardly rectifying conductances, and F , R and T had their usual meaning), or through fits to steady-state currents using Boltzmann combined to Goldman equations, the Goldman equation modelling currents through open channels ($I_{ss} = [G_l*V*(1-\exp(F*(V-E_{rev})/R/T))/(1-\exp(F*V/R/T)]/(1+\exp(z*F(V-E_{a50})/R/T)$ (Véry *et al.*, 1995), where G_l was the limit conductance at voltages infinitely negative (in inwardly rectifying conductances) or infinitely positive (in outwardly rectifying conductances)). When the concentration of permeant ions was almost the same on both sides of the membrane, $I = G*(V-E_{rev})$ replaced the Goldman equation for modelling currents through open channels.

For determination of K^+ transport affinity, a Michaelis-Menten equation was fitted to G_l values (obtained by the Goldman combined to Boltzmann fits to steady state currents) plotted against the K^+ concentration ($G_l = G_{lmax}*[K^+]/(K_M + [K^+])$).

The permeability ratios of different monovalent ions in K^+ and anionic conductances were determined using sets of external solutions containing a single permeant ion species and the Hodgkin and Katz 1949's equation, simplified as follows (Hille, 2001): $\Delta E_{rev} = E_{rev,A} - E_{rev,B} = (R*T/z*F)*\ln(P_A*[A]_o/P_B*[B]_o)$, where $E_{rev,A}$ and $E_{rev,B}$ are reversal potentials of currents determined with the ion A or B outside, P_A and P_B are the membrane permeabilities to ions A or B, respectively, $[A]_o$ and $[B]_o$ are the extracellular activities of ions A or B, and z was the ion valence.

ACKNOWLEDGEMENTS

We are grateful to Julie Cullimore and Clare Gough for critical reading of the manuscript. This work was supported in part by an ANR grant (ANR-11-BSV7-010-02) (to H.S.), and a doctoral grant of the China Scholarship Council to M.-Y.G.

CONFLICT OF INTEREST

The authors declare that there is no conflict of interest.

SUPPORTING INFORMATION

Figure S1. Comparison of the cation selectivity and the pH sensitivity of the two *M. truncatula* root hair outwardly rectifying K⁺-permeable conductances.

Figure S2. Affinity for K⁺ of the Shaker-like inwardly rectifying conductance of *M. truncatula* root hairs.

Figure S3. Effect of external Cl⁻ concentration on mean current-voltage relationships of S-type and hyperpolarization-activated anion conductances.

Figure S4. NO₃⁻ versus Cl⁻ selectivity of the hyperpolarization-activated anion conductance from *M. truncatula* root hairs.

Figure S5. Frequency of the different K⁺ conductances recorded at high cytosolic Ca²⁺ concentration.

Table S1. Pipette solutions used to study the different ionic conductances.

REFERENCES

- Ache, P., Becker, D., Ivashikina, N., Dietrich, P., Roelfsema, MR. and Hedrich, R.** (2000) GORK, a delayed outward rectifier expressed in guard cells of *Arabidopsis thaliana*, is a K⁺-selective, K⁺-sensing ion channel. *FEBS Lett.* **486**, 93–98.
- Ali, R., Ma, W., Lemtiri-Chlieh, F., Tsaltas, D., Leng, Q., von Bodman, S. and Berkowitz, GA.** (2007) Death don't have no mercy and neither does calcium: Arabidopsis CYCLIC NUCLEOTIDE GATED CHANNEL2 and innate immunity. *Plant Cell* **19**, 1081–1095.
- Barbier-Brygoo, H., Vinauger, M., Colcombet, J., Ephritikhine, G., Frachisse, J.-M. and Maurel, C.** (2000) Anion channels in higher plants: functional characterization, molecular structure and physiological role. *Biochim. Biophys. Acta* **1465**, 199–218.
- Bouteau, F., Pennarun, A.-M., Kurkdjian, A., Convert, M., Cornel, D., Monestiez, M., Rona, J.-P. and Bousquet, U,** (1999) Ion channels of intact young root hairs from *Medicago sativa*. *Plant. Physiol. Biochem.* **37**, 889–898.
- de Carvalho-Niebel, F., Lescure, N., Cullimore, J.V. and Gamas, P.** (1998) The *Medicago truncatula* *MtAnn1* gene encoding an annexin is induced by Nod factors and during the symbiotic interaction with *Rhizobium meliloti*. *Mol. Plant Microbe Interact.* **11**, 504–513.
- Damiani, I., Drain, A., Guichard, M., Balzergue, S., Boscari, A., Boyer, J.-C., Brunaud, V., Cottaz, S., Rancurel, C., DaRocha, M., Fizames, C., et al.** (2016) Nod factor effects on root hair-specific transcriptome of *Medicago truncatula*: Focus on plasma membrane transport systems and reactive oxygen species networks. *Frontiers Plant Sci.* **7**, 794.

- Dauphin, A., El Maarouf, H., Vienney, N., Rona, J.-P. and Bouteau, F. (2001) Effect of desiccation on potassium and anion currents from young root hairs: Implication on tip growth. *Physiol. Plant.* **113**, 79–84.
- Davenport, R.J. and Tester, M. (2000) A weakly voltage-dependent, nonselective cation channel mediates toxic sodium influx in wheat. *Plant Physiol.* **122**, 823–834.
- Davies, J.M. (2014) Annexin-mediated calcium signalling in plants. *Plants* **3**, 128-140.
- Demidchik, V., Davenport, R.J. and Tester, M. (2002) Nonselective cation channels in plants. *Annu. Rev. Plant Biol.* **53**, 67–107.
- Demidchik, V. and Tester, M. (2002) Sodium fluxes through nonselective cation channels in the plasma membrane of protoplasts from *Arabidopsis* roots. *Plant Physiol.* **128**, 379–387.
- Diatloff, E., Peyronnet, R., Colcombet, J., Thomine, S., Barbier-Brygoo, H. and Frachisse, J.-M. (2010) R type anion channel - A multifunctional channel seeking its molecular identity. *Plant Signal Behav.* **5**, 1347-1352.
- Downey, P., Szabo, I., Ivashikina, N., Negro, A., Guzzo, F., Ache, P., Hedrich, R., Terzi, M. and Schiavo, F.L. (2000) KDC1, a novel carrot root hair K⁺ channel. *J. Biol. Chem.* **275**, 39420–39426.
- Duby, G., Hosy, E., Fizames, C., Alcon, C., Costa, A., Sentenac, H. and Thibaud, J.-B. (2008) AtKC1, a conditionally targeted Shaker-type subunit, regulates the activity of plant K⁺ channels. *Plant J.* **53**, 115-123.
- Ehrhardt, D.W., Atkinson, E.M. and Long, S.R. (1992) Depolarization of alfalfa root hair membrane potential by *Rhizobium meliloti* Nod factors. *Science* **256**, 998–1000.
- Elzenga, J.T.M. and Vanvolkenburgh, E. (1997) Kinetics of Ca²⁺- and ATP dependent, voltage-controlled anion conductance in the plasma membrane of mesophyll cells of *Pisum sativum*. *Planta* **201**, 415–423.
- Fahraeus, G. (1957) The infection of clover root hairs by nodule bacteria studied by a simple glass slide technique. *J. Gen. Microbiol.* **16**, 374-381.
- Felle, H.H. and Hepler, P.K. (1997) The cytosolic Ca²⁺ concentration gradient of *Sinapis alba* root hairs as revealed by Ca²⁺-selective microelectrode tests and Fura-Dextran ratio imaging. *Plant Physiol.* **114**, 39-45.
- Felle, H.H., Kondorosi, E., Kondorosi, A. and Schultze, M. (1995) Nod signal-induced plasma membrane potential changes in alfalfa root hairs are differentially sensitive to structural modifications of the lipochitoooligosaccharide. *Plant J.* **7**, 939–947.
- Felle, H.H., Kondorosi, E., Kondorosi, A. and Schultze, M. (1998) The role of ion fluxes in Nod-factor signaling in *Medicago sativa*. *Plant J.* **13**, 455-463.
- Forestier, C., Bouteau, F., Leonhardt, N., and Vavasseur, A. (1998) Pharmacological properties of slow anion currents in intact guard cells of *Arabidopsis*. Application of the discontinuous single-electrode voltage-clamp to different species. *Pflügers Arch.* **436**, 920–927.
- Frachisse, J.-M., Thomine, S., Colcombet, J., Guern, J. and Barbier-Brygoo, H. (1999) Sulphate is both a substrate and an activator of the voltage-dependent anion channel of *Arabidopsis* hypocotyl cells. *Plant Physiol.* **121**, 253-261.

- Frachisse, J.-M., Colcombet, J., Guern, J. and Barbier-Brygoo, H.** (2000) Characterization of a nitrate-permeable channel able to mediate sustained anion efflux in hypocotyl cells from *Arabidopsis thaliana*. *Plant J.* **21**, 361–371.
- Gassmann, W. and Schroeder, J.I.** (1994) Inward-rectifying K⁺ channels in root hairs of wheat: A mechanism for aluminium-sensitive low-affinity K⁺ uptake and membrane potential control. *Plant Physiol.* **105**, 1399–1408.
- Gaymard, F., Pilot, G., Lacombe, B., Bouchez, D., Bruneau, D., Boucherez, J., Michaux-Ferriere, N., Thibaud, J.-B. and Sentenac, H.** (1998) Identification and disruption of a plant Shaker-like outward channel involved in K⁺ release into the xylem sap. *Cell* **94**, 647–655.
- Geiger, D., Becker, D., Vosloh, D., Gambale, F., Palme, K., Rehers, M., Anschuetz, U., Dreyer, I., Kudla, J. and Hedrich, R.** (2009a) Heteromeric AtKC1·AKT1 channels in *Arabidopsis* roots facilitate growth under K⁺-limiting conditions. *J. Biol. Chem.* **284**, 21288–21295.
- Geiger, D., Scherzer, S., Mumm, P., Stange, A., Marten, I., Bauer, H., Ache, P., Matschi, S., Liese, A., Al-Rasheid, K.A., et al.** (2009b) Activity of guard cell anion channel SLAC1 is controlled by drought-stress signaling kinase-phosphatase pair. *Proc. Natl. Acad. Sci. USA* **106**, 21425–21430.
- Geiger, D., Maierhofer, T., Al-Rasheid, K.A., Scherzer, S., Mumm, P., Liese, A., Ache, P., Wellmann, C., Marten, I., Grill, E., et al.** (2011) Stomatal closure by fast abscisic acid signaling is mediated by the guard cell anion channel SLAH3 and the receptor RCAR1. *Sci. Signal.* **4**, ra32.
- Gutermuth, T., Lassig, R., Portes, M.T., Maierhofer, T., Romeis, T., Borst, J.W., Hedrich, R., Feijó, J.A. and Konrad, K.R.** (2013) Pollen tube growth regulation by free anions depends on the interaction between the anion channel SLAH3 and calcium-dependent protein kinases CPK2 and CPK20. *Plant Cell* **25**, 4525–4543.
- Guzel Deger, A., Scherzer, S., Nuhkat, M., Kedzierska, J., Kollist, H., Brosch, M., Unyayar, S., Boudsocq, M., Hedrich, R. and Roelfsema, M.R.G.** (2015) Guard cell SLAC1-type anion channels mediate flagellin-induced stomatal closure. *New Phytol.* **208**, 162–173.
- Hartje, S., Zimmermann, S., Klonus, D. and Mueller-Roeber, B.** (2000) Functional characterisation of LKT1, a K⁺-uptake channel from tomato root hairs, and comparison with the closely related potato inwardly rectifying K⁺-channel SKT1 after expression in *Xenopus* oocytes. *Planta*, **210**, 723–731.
- Hedrich, R.** (2012) Ion channels in plants. *Physiol. Rev.* **92**, 1777–1811.
- Hedrich, R. and Marten, I.** (1993) Malate-induced feedback regulation of plasma membrane anion channels could provide a CO₂ sensor to guard cells. *EMBO J.* **12**, 897–901.
- Hosy, E., Vavasseur, A., Mouline, K., Dreyer, I., Gaymard, F., Porée, F., Boucherez, J., Lebaudy, A., Bouchez, D., Véry, A.-A., et al.** (2003) The *Arabidopsis* outward K⁺ channel *GORK* is involved in regulation of stomatal movements and plant transpiration. *Proc. Natl. Acad. Sci. USA* **100**, 5549–5554.

- Hosy, E., Duby, G., Véry, A.-A., Costa, A., Sentenac, H. and Thibaud, J.-B.** (2005) A procedure for localisation and electrophysiological characterisation of ion channels heterologously expressed in a plant context. *Plant Methods* **1**, 14.
- Ivashikina, N., Becker, D., Ache, P., Meyerhoff, O., Felle, H.H. and Hedrich, R.** (2001) K⁺ channel profile and electrical properties of *Arabidopsis* root hairs. *FEBS Lett.* **508**, 463-469.
- Jammes, F., Hu, H.-C., Villiers, F., Bouten, R. and Kwak, J.M.** (2011) Calcium-permeable channels in plant cells. *FEBS J.* **278**, 4262–4276 .
- Johansson, I., Wulfetang, K., Porée, F., Michard, E., Gajdanowicz, P., Lacombe, B., Sentenac, H., Thibaud, J.-B., Mueller-Roeber, B., Blatt, M.R. and Dreyer, I.** (2006) External K⁺ modulates the activity of the *Arabidopsis* potassium channel SKOR via an unusual mechanism. *Plant J.* **46**, 269-281.
- Kodavali, P.K., Skowronek, K., Koszela-Piotrowska, I., Strzelecka-Kiliszek, A., Pawlowski, K. and Pikula, S.** (2013) Structural and functional characterization of annexin 1 from *Medicago truncatula*. *Plant Physiol. Biochem.* **73**, 56-62.
- Köhler, B.** (2007) Step by step: Deciphering ion transport in the root xylem parenchyma. *Plant Signal Behav.* **2(4)**, 303-305.
- Köhler, B. and Raschke, K.** (2000) The delivery of salts to the xylem: three types of anion conductance in the plasmalemma of the xylem parenchyma of roots of barley. *Plant Physiol.* **122**, 243–254.
- Kong, D., Hu, H.-C., Okuma, E., Lee, Y., Lee, H.S., Munemasa, S., Cho, D., Ju, C., Pedoeim, L., Rodriguez, B., et al.** (2016) L-Met activates *Arabidopsis* GLR Ca²⁺ channels upstream of ROS production and regulates stomatal movement. *Cell Rep.* **17**, 2553–2561.
- Kurkdjian, A., Bouteau, F., Pennarun, A.-M., Convert, M., Cornel, D., Rona, J.-P. and Bousquet, U.** (2000) Ion currents involved in early Nod factor response in *Medicago sativa* root hairs: a discontinuous single-electrode voltage-clamp study. *Plant J.* **22**, 9-17.
- Langer, K., Ache, P., Geiger, D., Stinzinger, A., Arend, M., Wind, C., Regan, S., Fromm, J. and Hedrich, R.** (2002) Poplar potassium transporters capable of controlling K⁺ homeostasis and K⁺-dependent xylogenesis. *Plant J.* **32**, 997–1009.
- Laohavisit, A., Shang, Z., Rubio, L., Cuin, T.A., Véry, A.-A., Wang, A., Mortimer, J.C., Macpherson, N., Coxon, K.M., Battey, N.H., et al.** (2012) *Arabidopsis* Annexin1 mediates the radical-activated plasma membrane Ca²⁺- and K⁺-permeable conductance in root cells. *Plant Cell* **24**, 1522–1533.
- Lew, R.R.** (1991) Substrate regulation of single potassium and chloride ion channels in *Arabidopsis* plasma membrane. *Plant Physiol.* **95**, 642–647.
- Ligaba, A., Maron, L., Shaff, J., Kochain, L. and Piñeros, M.** (2012) Maize ZmALMT2 is a root anion transporter that mediates constitutive root malate efflux. *Plant Cell Environ.* **35**, 1185–1200.
- Long, S.R.** (1996). *Rhizobium* symbiosis: Nod factors in perspective. *Plant Cell* **8**, 1885–1898.
- Maierhofer, T., Lind, C., Hüttel, S., Scherzer, S., Papenfuß, M., Simon, J., Al-Rasheid, K.A.S., Ache, P., Rennenberg, H., Hedrich, R., et al.** (2014) A single-pore residue

renders the *Arabidopsis* root anion channel SLAH2 highly nitrate selective. *Plant Cell*, **26**, 2554-2567.

- Meyer, S., Mumm, P., Imes, D., Endler, A., Weder, B., Al-Rasheid, K.A., Geiger, D., Marten, I., Martinoia, E. and Hedrich, R.** (2010) AtALMT12 represents an R-type anion channel required for stomatal movement in *Arabidopsis* guard cells. *Plant J.* **63**, 1054–1062.
- Miedema, H., Demidchik, V., Véry, A.-A., Bothwell, J.H.F., Brownlee, C. and Davies, J.M.** (2008) Two voltage-dependent calcium channels co-exist in the apical plasma membrane of *Arabidopsis thaliana* root hairs. *New Phytol.* **179**, 378–385.
- Mori, I.C., Murata, Y., Yang, Y., Munemasa, S., Wang, Y.-F., Andreoli, S., Tiriach, H., Alonso, J.M., Harper, J.F., Ecker, J.R., et al.** (2006) CDPKs CPK6 and CPK3 function in ABA regulation of guard cell S-type anion- and Ca²⁺- permeable channels and stomatal closure. *Plos. Biol.* **4**(10), e327.
- Mumm, P., Imes, D., Martinoia, E., Al-Rasheid, K.A.S., Geiger, D., Marten, I. and Hedrich, R.** (2013) C-terminus-mediated voltage gating of *Arabidopsis* guard cell anion channel QUAC1. *Mol Plant* **6**, 550–1563.
- Osakabe, Y., Arinaga, N., Umezawa, T., Katsura, S., Nagamachi, K., Tanaka, H., Ohiraki, H., Yamada, K., Seo, S.-U., Abo, M., et al.** (2013) *Plant Cell* **25**, 609–624.
- Peterson, R.L. and Farquhar, M.L.** (1996) Root hairs: specialized tubular cells extending root surfaces. *Bot. Rev.* **6**, 21–40.
- Piñeros, M.A., Cançado, G.M.A., Maron, L.G., Lyi, S.M., Menossi, M. and Kochian, L.V.** (2008) Not all ALMT1-type transporters mediate aluminum activated organic acid responses: the case of ZmALMT1 – an anion-selective transporter. *Plant J.* **53**, 352–367.
- Piñeros, M.A. and Kochian, L.V.** (2003) Differences in whole-cell and single channel ion currents across the plasma membrane of mesophyll cells from two closely related *Thlaspi* species. *Plant Physiol.* **131**, 583–594.
- Reintanz, B., Szyroki, A., Ivashikina, N., Ache, P., Godde, M., Becker, D., Palme, K. and Hedrich, R.** (2002) AtKC1, a silent *Arabidopsis* potassium channel alpha -subunit modulates root hair K⁺ influx. *Proc. Natl. Acad. Sci. USA* **99**, 4079-4084.
- Roberts, S.K.** (2006) Plasma membrane anion channels in higher plants and their putative functions in roots. *New Phytol.* **169**, 647–666.
- Roelfsema, M.R.G., Hedrich, R. and Geiger, D.** (2012) Anion channels: master switches of stress responses. *Trends Plant Sci.* **17**, 221-229.
- Schmidt, C. and Schroeder, J.I.** (1994) Anion selectivity of slow anion channels in the plasma-membrane of guard-cells – large nitrate permeability. *Plant Physiol.* **106**, 383–391.
- Schroeder, J.I. and Keller, B.U.** (1992) Two types of anion channel currents in guard cells with distinct voltage regulation. *Proc. Natl. Acad. Sci. USA*, **89**, 5025–5029.
- Shabala, S., Demidchik, V., Shabala, L., Cuin, T.A., Smith, S.J., Miller, A.J., Davies, J.M. and Newman, I.A.** (2006) Extracellular Ca²⁺ ameliorates NaCl-induced K⁺ loss from *Arabidopsis* root and leaf cells by controlling plasma membrane K⁺-permeable channels. *Plant Physiol.* **141**, 1653–65.

- Thomine, S., Zimmermann, S., Guern, J. and Barbier-Brygoo, H.** (1995) ATP-dependent regulation of an anion channel at the plasma membrane of protoplasts from epidermal cells of *Arabidopsis* hypocotyls. *Plant Cell* **7**, 2091-2100.
- Vahisalu, T., Kollist, H., Wang, Y.-F., Nishimura, N., Chan, W.-Y., Valerio, G., Lamminmäki, A., M. Brosché, H. Moldau, R. Desikan, et al.** (2008) SLAC1 is required for plant guard cell S-type anion channel function in stomatal signalling. *Nature* **452**, 487–491.
- Véry, A.-A. and Davies, J.M.** (2000) Hyperpolarization-activated calcium channels at the tip of *Arabidopsis* root hairs. *Proc. Natl. Acad. Sci. USA*, **97**, 9801-9806.
- Véry, A.-A., Gaymard, F., Bosseux, C., Sentenac, H. and Thibaud, J.-B.** (1995) Expression of a cloned plant K⁺ channel in *Xenopus* oocytes: analysis of macroscopic currents. *Plant J.* **7**, 321-332.
- Véry, A.-A., Nieves-Cordones, M., Daly, M., Khan, I., Fizames, C. and Sentenac, H.** (2014) Molecular biology of K⁺ transport across the plant cell membrane: what do we learn from comparison between plant species? *J. Plant Physiol.* **171**, 748-769.
- Wang, Y., He, L., Li, H.D., Xu, J. and Wu, W.-H.** (2010) Potassium channel α -subunit AtKC1 negatively regulates AKT1-mediated K⁺ uptake in *Arabidopsis* roots under low-K⁺ stress. *Cell Res.* **20**, 826-837.
- Wang, Y.-F., Munemasa, S., Nishimura, N., Ren, H.-M., Robert, N., Han, M., Puzõrjova, I., Kollist, H., Lee, S., Mori, I. and Schroeder, J.I.** (2013) Identification of cyclic GMP-activated nonselective Ca²⁺-permeable cation channels and associated CNGC5 and CNGC6 genes in *Arabidopsis* guard cells. *Plant Physiol.* **163**, 578–590.
- Ward, J.M., Mäser, P. and Schroeder, J.I.** (2009) Plant ion channels: gene families, physiology, and functional genomics analyses. *Annu. Rev. Physiol.* **71**, 59–82.
- Wegner, L.H. and De Boer, A.H.** (1997) Properties of two outward rectifying channels in root xylem parenchyma cells suggest a role in K⁺ homeostasis and long distance signalling. *Plant Physiol.* **115**, 1707-1719.
- Wegner, L.H. and Raschke, K.** (1994) Ion channels in the xylem parenchyma of barley roots. A procedure to isolate protoplasts from this tissue and a patch clamp exploration of salt passages into xylem vessels. *Plant Physiol.* **105**, 799–813.
- White, P.J., Bowen, H.C., Demidchik, V., Nichols, C. and Davies, J.M.** (2002) Genes for calcium permeable channels in the plasma membrane of plant root cells. *Biochim. Biophys. Acta* **1564**, 299–309.
- Yuan, F., Yang, H., Xue, Y., Kong, D., Ye, R., Li, C., Zhang, J., Theprungsirikul, L., Shrift, T., Krichilsky, B., et al.** (2014) OSCA1 mediates osmotic stress-evoked Ca²⁺ increases vital for osmosensing in *Arabidopsis*. *Nature* **514**, 367-371.
- Zhang, W.-H., Ryan, P.R., Sasaki, T., Yamamoto, Y., Sullivan, W., Tyerman and S.D.** (2008) Characterization of the TaALMT1 protein as an Al³⁺-activated anion channel in transformed tobacco (*Nicotiana Tabacum* L.) cells. *Plant Cell Physiol.* **49**, 1316–1330.
- Zhang, W.-H., Ryan, P.R. and Tyerman, S.D.** (2004a) Citrate-permeable channels in the plasma membrane of cluster roots from white lupin. *Plant Physiol.* **136**, 3771–3783.

- Zhang, W.-H., Walker, N.A., Tyerman, S.D. and Patrick, J.W.** (2000) Fast activation of a time-dependent outward current in protoplasts derived from coats of developing *Phaseolus vulgaris* seeds. *Planta* **211**, 894–898.
- Zhang, W.-H., Skerrett, M., Walker, N.A., Patrick, J.W. and Tyerman, S.D.** (2002) Nonselective currents and channels in plasma membranes of protoplasts from coats of developing seeds of bean. *Plant Physiol.* **128**, 388-399.
- Zhang, W.-H., Walker, N.A., Tyerman, S.D. and Patrick, J.W.** (2004b) Pulsing Cl^- currents in seed coat cells of developing bean seeds linked to hyperosmotic turgor regulation. *J. Exp. Bot.* **55**, 993–1001.
- Zimmermann, S., Talke, I., Ehrhardt, T., Nast, G. and Müller-Röber, B.** (1998) Characterization of SKT1, an inwardly rectifying potassium channel from potato by heterologous expression in insect cells. *Plant Physiol.* **116**, 879–890.

FIGURE LEGENDS

Figure 1. Activation kinetics and voltage dependence of two *M. truncatula* root hair outward conductances in K^+ -containing solutions.

(a) Voltage-clamp “activation” protocol.

(b-i) Patch-clamp experiments were performed in the whole-cell mode on root hair protoplasts isolated by enzymatic treatment.

(b, d, f, h) Fast-activating outward conductance.

(c, e, g, i) Shaker-like outward conductance.

(b, c) Current activation kinetics.

The bath solution contained 30 mM K-gluconate, 1 mM CaCl_2 , 10 mM Mes/Tris (pH 5.6) and the pipette solution contained 150 mM K-gluconate, 10 mM EGTA, 2 mM MgCl_2 , 2 mM Mg-ATP, 10 mM HEPES/Tris (pH 7.4). The osmolarity of bath and pipette solutions was adjusted to 290 and, respectively, 300 mosmol/L with D-sorbitol.

(d, e) Current-voltage (I-V) relationships at steady state.

(f, g) Effect of varying external K^+ concentration (3, 10, 30 or 100 mM K-gluconate) on I-V relationships. The voltage-clamp protocol was similar to that shown in (a), however, the holding voltage was more negative when the K^+ concentration was lower. Currents sampled at the end of activation voltage pulses were normalized by the value recorded at +45 mV (f) and +60 mV (g) in the 30 mM K^+ solution. Data are means \pm SE ($n = 3$ to 5 in (f), and $n = 4$ to 6 in (g)). The solid lines in (f) display combined Goldman and Boltzmann equation fits to I-V data (z and E_{a50} were hypothesized to be independent of the external K^+ concentration).

(h, i) Open probability (P_o) regulation by voltage. (h) $P_o/P_{o\text{max}}$ values for the fast-activating conductance were obtained by dividing the mean steady-state currents displayed in (f) by the mean diffusive currents (Goldman equation) estimated from the steady-state current fit. The solid line was drawn with Boltzmann parameters obtained from the fit: z (equivalent gating charge) = 0.17, E_{a50} (half activation potential) = +33 mV. (i) $P_o/P_{o\text{max}}$ values for the

Shaker-like outward conductance, from one representative protoplast. Initial deactivation currents (I_{tail}) recorded upon return to the holding potential after the activation steps were plotted against the voltage of the activation steps. Boltzmann equations were adjusted to the latter relationships, with the same z for all K^+ concentrations: $z = 1.27$, $E_{a50} = -25, -6, 13$ and 40 mV in $3, 10, 30$ and 100 mM K^+ , respectively. $P_o/P_{o,max}$ vs voltage relationships were obtained by dividing I_{tail} data by the maximal value of I_{tail} extrapolated from the Boltzmann fits. Solid lines were drawn with Boltzmann parameters obtained from the fits.

Figure 2. Reversal potential of two *M. truncatula* root hair outwardly rectifying conductances in K^+ -containing solutions.

(a) Example of voltage-clamp “tail current” protocol used for the determination of the reversal potential of currents.

(b, d, f) Fast-activating outwardly rectifying conductance.

(c, e, g) Shaker-like outwardly rectifying conductance.

(b, c) Representative traces of currents recorded using the “tail current” protocol in the presence of 30 mM external K^+ (same bath and pipette solutions as in Figure 1b, c). A zoom on tail currents (dashed circle) is displayed on the right of each panel. The arrows mark the position of zero current through the outwardly rectifying conductances.

(d, e) Difference between initial and final tail currents ($I_i - I_f$ tail) plotted against the voltage, for determination of the reversal potential of currents (E_{rev}). The K^+ equilibrium potential (E_K) was -37 mV.

(f, g) Variation of E_{rev} with the external K^+ activity. Data are means \pm SE ($n \geq 4$). The solid lines show a logarithmic fit to E_{rev} data, while the dashed lines indicate the K^+ equilibrium potential.

Figure 3. Activation kinetics and voltage dependence of a root hair inwardly rectifying conductance in a K^+ -containing solution.

(a) Voltage-clamp “activation” protocols (top) and kinetics of Shaker-like inwardly rectifying current activation (bottom). Whole-cell patch-clamp experiments were performed on root hair protoplasts isolated by enzymatic treatment. The osmolarity of the bath and pipette solutions was adjusted to 280 and 300 mosmol/L, respectively, with D-sorbitol. Shaker-like currents were recorded using a bath solution containing 30 mM K-gluconate, 10 mM $CaCl_2$ and 10 mM Mes/Tris (pH 5.6), and a pipette solution identical to that in Figure 1.

(b) I-V relationships drawn from steady state currents shown in (a).=

Figure 4. Selectivity analyses of the Shaker-like inward conductance.

(a) Example of “tail current” protocol used for determination of the reversal potential of Shaker-like inward currents (top) and representative current traces recorded using the “tail current” protocol (bottom). Bath and pipette solutions used for the Shaker-like inward conductance were the same as in Figure 3c. A zoom on tail currents (dashed circle) is displayed on the right of bottom panel. The arrows mark the position of zero current through the analyzed conductance.

(b) Difference between initial and final tail currents (I_i - I_f tail) plotted against the voltage, for determination of E_{rev} . E_K was -37 mV.

(c) Variation of E_{rev} with the external K^+ activity. Currents were successively recorded in external solutions containing 3, 10, 30 or 100 mM K-gluconate, and an ionic background of 1 mM $CaCl_2$ and 10 mM Mes/Tris (pH 5.6). The osmolarity of the bath was adjusted to 280 mosmol/L with D-sorbitol. The pipette solution was the same as in Figure 3c. Data are mean \pm SE ($n = 3$ to 8). The solid line shows a logarithmic fit to E_{rev} data, while the dashed line indicates the K^+ equilibrium potential.

Figure 5. Activation kinetics and voltage dependence of two *M. truncatula* root hair anion conductances.

(a, b) Voltage-clamp protocols used for the analysis of S-type (c, e, g) and, respectively, hyperpolarization-activated (d, f h) anion conductances. Whole-cell patch-clamp experiments were performed on root hair protoplasts isolated by enzymatic treatment. The external solution contained 10 mM $CaCl_2$, 80 mM TEA-Cl, 10 mM Hepes/Tris (pH 7.5), and 100 mM D-sorbitol. The pipette solution was composed of 100 mM TEA-Cl, 2 mM $MgCl_2$, 2 mM Mg-ATP, 5 mM EGTA, 4.65 mM $CaCl_2$ (free Ca^{2+} 1 μ M), 10 mM Hepes/Tris (pH 7.4), and 90 mM D-Sorbitol.

(c, d) Representative current traces. Anion currents were recorded 7 to 10 minutes after whole-cell access.

(e, f) Current-voltage relationships, at the end of the 10 s voltage pulses. The position of the equilibrium potential for Cl^- (E_{Cl}) is indicated by the arrow. In (e), the solid line shows a fit to currents by the function $I = G \cdot (V - E_{rev}) \cdot P_o / P_o,max$, where G is the macroscopic conductance when the channels are open, and $P_o / P_o,max$ follows a Boltzmann distribution ($P_o / P_o,max = 1 / (1 + \exp(z \cdot F \cdot (-V + E_{a50}) / R / T))$; $z = 0.21$, $E_{a50} = -158$ mV).

(g, h) Voltage gating. (g) The relative open probabilities were determined from the fit to I-V data shown in (e). The solid line shows the Boltzmann fit. (h) The maximal hyperpolarization-activated currents recorded between +45 and -150 mV (insert) were fitted (solid line) with the same functions as in (e), however using a Boltzmann distribution in opposite direction ($I = G \cdot (V - E_{rev}) / (1 + \exp(z \cdot F \cdot (V - E_{a50}) / R / T))$; $z = 0.20$, $E_{a50} = -41$ mV).

Figure 6. Sensitivity of S-type (a, c) and hyperpolarization-activated (b, d) anion conductances to external Cl^- .

The voltage-clamp protocols were similar to those shown in Figure 5a, b. Whole cell currents were measured at the end of the 10 s pulses.

(a, b) I-V relationships from representative protoplasts, in the presence of 20 or 100 mM external Cl^- concentrations. The pipette solution and the external solution containing 100 mM Cl^- were those given in the legend to Figure 5. The external solution containing 20 mM Cl^- was composed of the same salts except TEA-Cl, the removal of which was osmotically compensated by D-sorbitol. Currents were recorded successively with both bath solutions on the same protoplasts.

(c, d) Variation of the reversal potential of currents with the logarithm of the external Cl^- activity. E_{rev} values were obtained from I-V relationships. Data are means \pm SE ($n = 3$ in (c), and $n = 4$ in (d)). The solid lines show logarithmic fits to experimental data, while the dashed lines indicate E_{Cl^-} .

Figure 7. Effect of the cytosolic Ca^{2+} concentration on the inward and outward K^+ conductances of enzymatically-isolated root hair protoplasts.

Currents were recorded 10 to 20 min after whole cell access in the presence of 30 mM K^+ in the bath solution (same solution as in Figure 1b, c).

(a, d) Shaker-like inwardly rectifying conductance

(b, e) Shaker-like outwardly rectifying conductance

(c, f) Cationic fast activating outward conductance

(a-c) Representative recordings of the three cationic conductances at high cytosolic Ca^{2+} concentration. The pipette solution, which contained 150 mM K^+ was identical to that described in Figure 1 except that 4.65 mM CaCl_2 were added to increase the free Ca^{2+} concentration in the cytosol to 1 μM (Table S1).

(d-f) Comparison of I-V relationships of the three cationic conductances at low and high cytosolic Ca^{2+} concentrations. Currents were measured at steady state. The pipette solution with low Ca^{2+} concentration (<10 nM) was that described in Figure 1. Data are means \pm SE ($n = 10$ in (d), $n = 5$ and 4 at low and high Ca^{2+} , respectively in (e), and $n = 5$ in (f)).

Figure 8. Frequency of the different K^+ conductances recorded at low cytosolic Ca^{2+} concentration.

Protoplasts were isolated enzymatically. The external medium contained 30 mM K^+ . Bath and pipette solutions were those described in the legend to Figure 1b, c. The surface of each rectangle is proportional to the number of protoplasts in which the corresponding current type was observed.

Figure 9. Ionic conductances in spheroplasts of young root hair apical membrane, isolated by laser cell-wall ablation.

(a) Recovery of *M. truncatula* root hair spheroplasts by laser microdissection. (Left) Root hair plasmolysis after 3 min in 350 mosmol.L⁻¹ solution. The arrow points to the plasma membrane retracted from the cell wall. (Middle) The apical cell-wall of a plasmolyzed root hair was cut with the laser. (Right) Spheroplast of apical root hair membrane extruded upon deplasmolysis in 275 mosmol.L⁻¹ solution).

(b-f) Similar ionic conductances to those described in enzymatically-isolated protoplasts, observed in young root hair spheroplasts: example of current traces (top) and corresponding I-V relationships (bottom). The Shaker-like inward K^+ conductance (b), fast-activating outward cationic conductance (c) and the Shaker-like outward K^+ conductance (d) were recorded in the presence of 30 mM K^+ -gluconate (pH 5.6) externally, and 150 mM K^+ -gluconate (pH 7.4) internally (same solutions as in Figure 1). S-type anion currents (e) and hyperpolarization-activated anion currents (f) were recorded in the presence of 100 mM external and 113 mM internal Cl^- (same bath and pipette solutions as in Figure 5).

Figure 10. Candidate genes coding for the identified *M. truncatula* root hair conductances. Proposed candidate genes are based on *M. truncatula* root hair RNA-seq analysis (Damiani *et al.*, 2016) and functional information available on characterized members from the corresponding gene families in other plant species (Geiger *et al.*, 2009; Jammes *et al.*, 2011; Meyer *et al.*, 2010; Davies, 2014; Véry *et al.*, 2014).

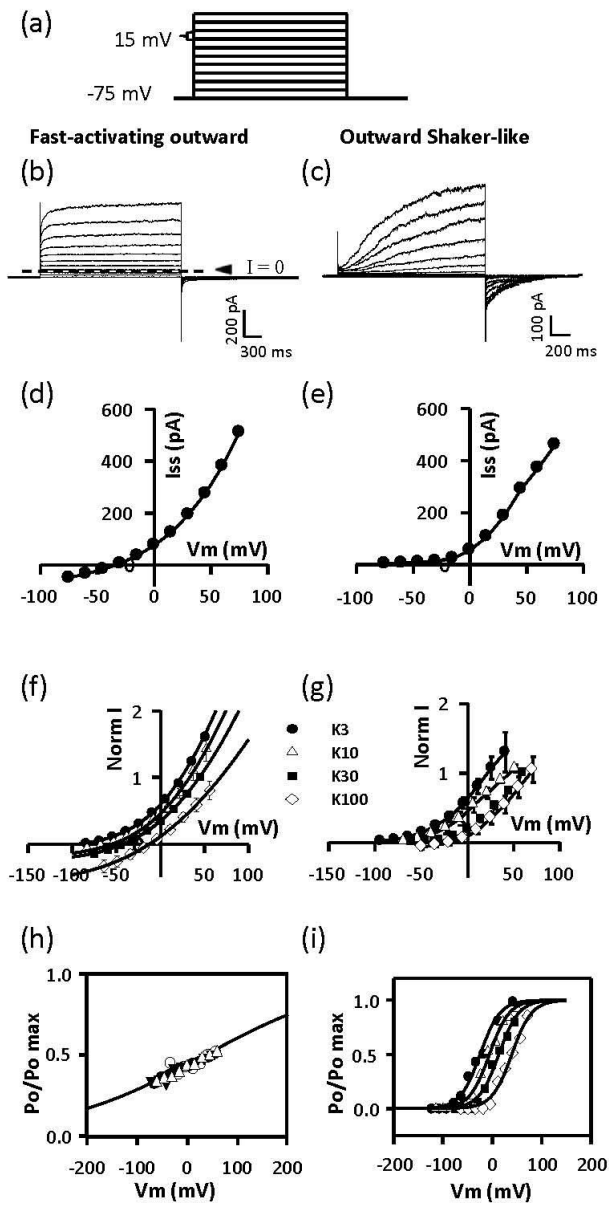


Figure 1

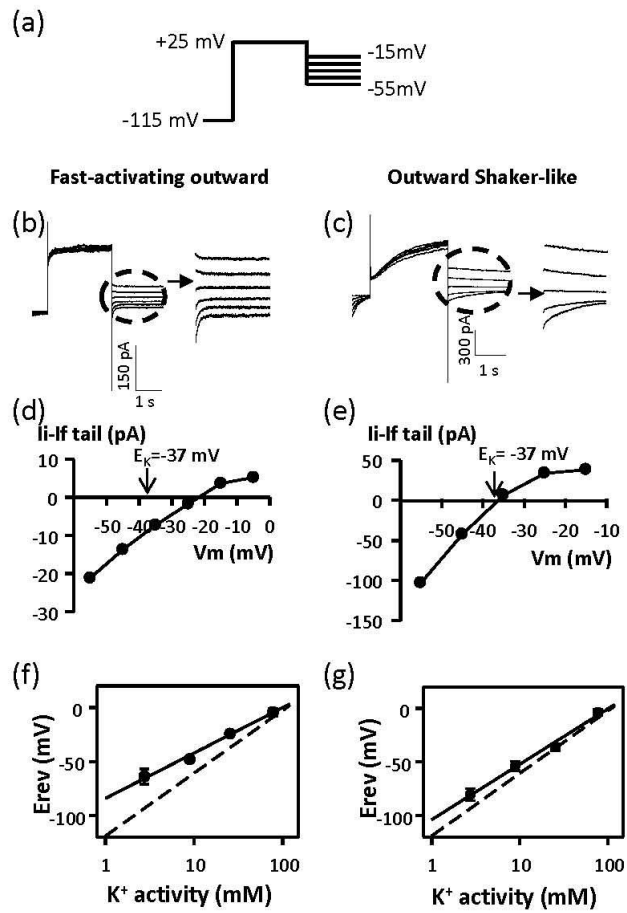


Figure 2

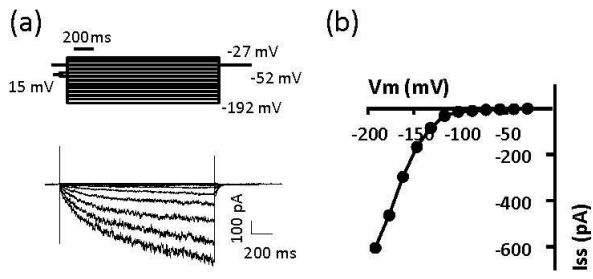


Figure 3

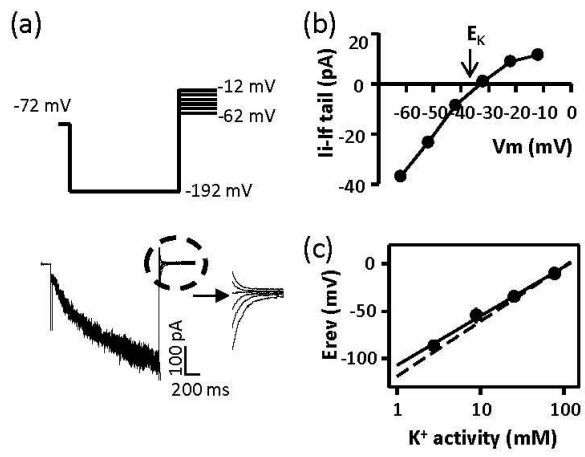


Figure 4

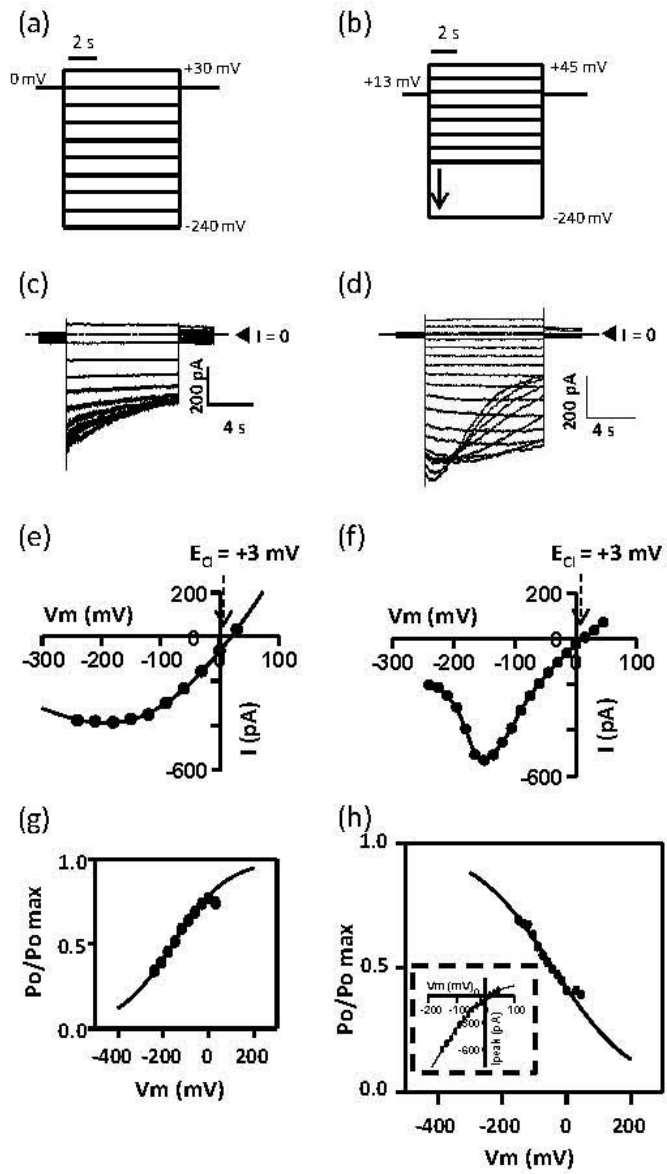


Figure 5

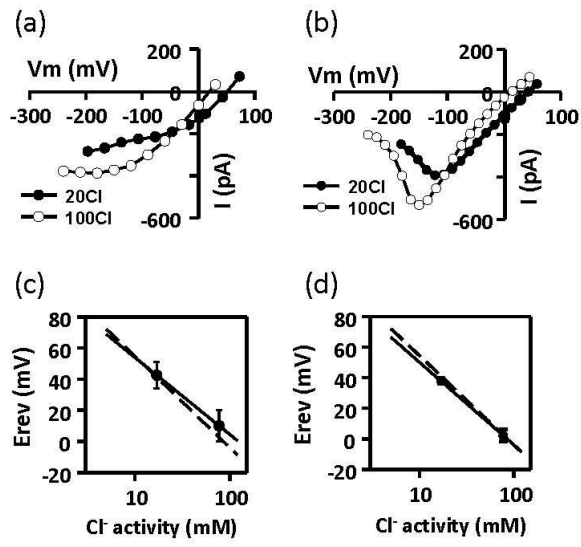


Figure 6

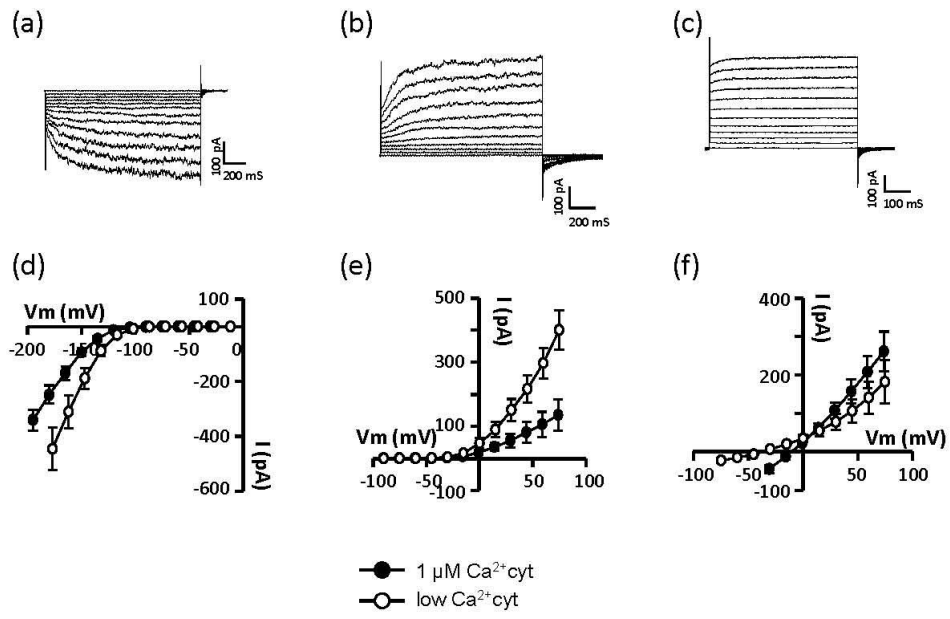


Figure 7

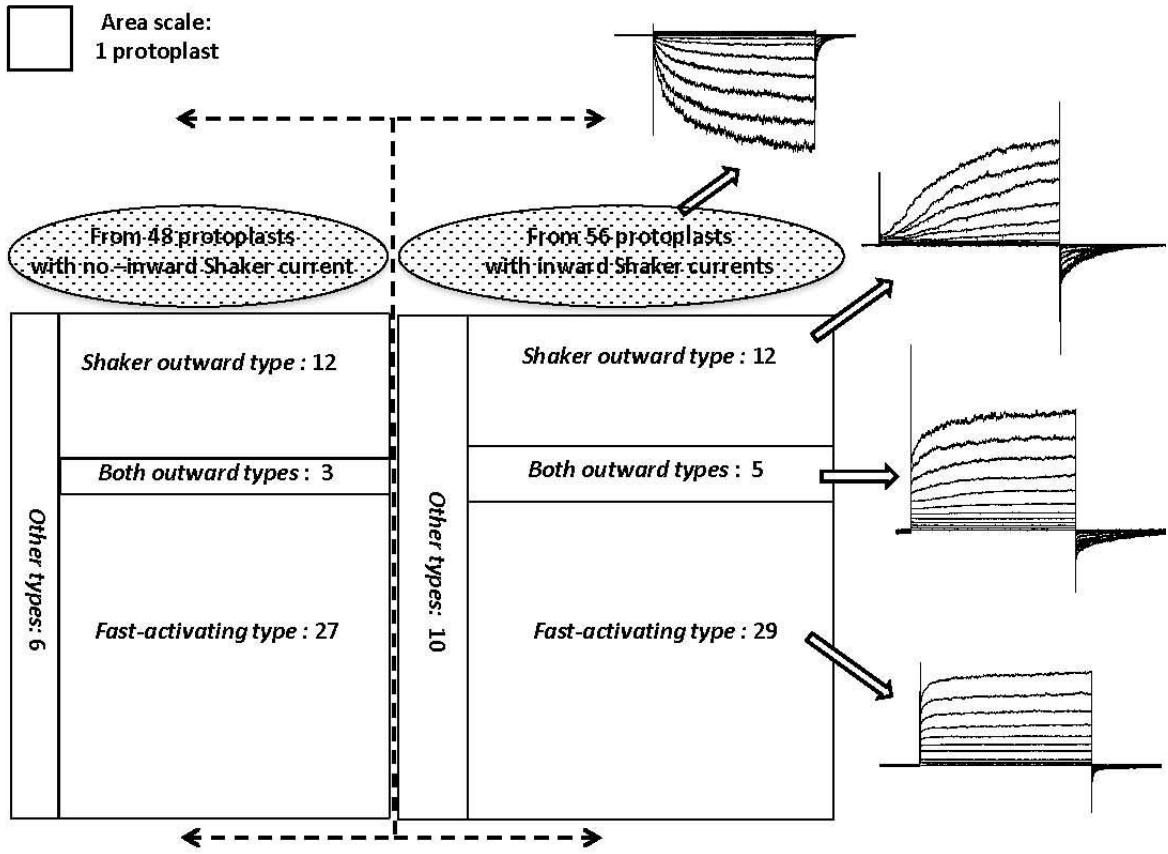


Figure 8

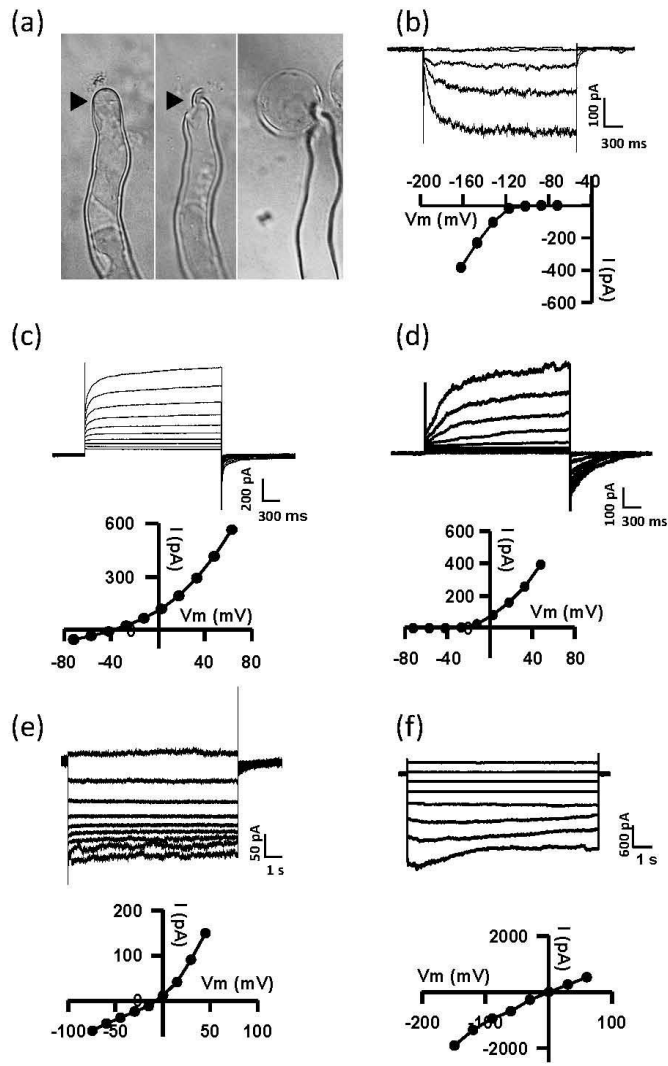


Figure 9

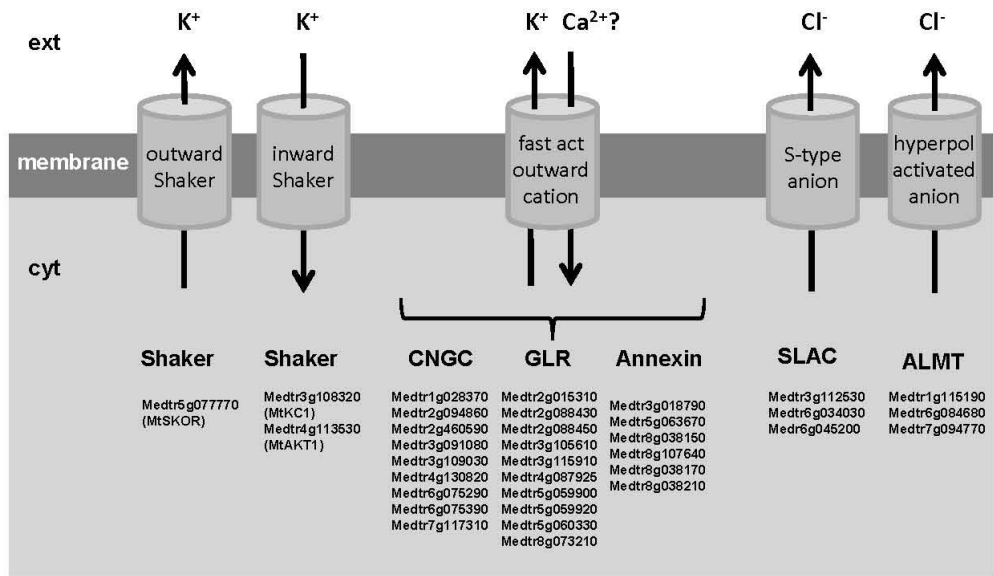


Figure 10